

## Oxidation of Ground Tire Rubber for Ammonia Adsorbents

Sirinapa Mayod<sup>1)</sup> Sutamma Tanasarn<sup>2)</sup> and Supitcha Rungrodmitchai<sup>3)\*</sup>

Department of Chemical Engineering, Thammasat school of engineering,

Thammasat University, Phatum Thani 12120, Thailand.

\*Corresponding author. E-mail address: supitcha@engr.tu.ac.th

### Abstract

In this study, ground tire rubber (average particle size = 456  $\mu\text{m}$ ) was successfully modified by oxidation reaction using an acid mixture of the  $\text{HNO}_3/\text{H}_3\text{PO}_4/\text{NaNO}_2$  system, for which the ratio of nitric acid and phosphoric was 1:3 and the concentration of sodium nitrite was 1.4% w/v. Scanning electron microscopy and BET surface area analyses revealed that the modified ground tire rubber (M-GTR) became more porous and had larger surface area than the raw ground tire rubber (R-GTR). For kinetic study, M-GTR agreed with pseudo-second order model. In case of isotherm study, R-GTR was fitted well with Langmuir isotherm while M-GTR was suitable with both Langmuir and Freundlich isotherms. Moreover, the maximum ammonia adsorption capacities from the Langmuir isotherm of R-GTR and M-GTR were found to be 12.59 and 44.25 mg/g, respectively.

**Keywords:** ground tire rubber, chemical modification, adsorbent, oxidation, ammonia adsorption,

### 1. Introduction

In fish ponds, ammonia is generated from the excretion of fish. The rate of ammonia excretion depends on the feeding rate and the protein in the feed. Ammonia is toxic to fish and the ecosystem [1, 2]. With the accumulation in ponds, fish cannot extract energy from the feed efficiently, and the toxic levels of ammonia in the pond can lead to death. The nitrification by bacteria converts ammonia to nitrite ( $\text{NO}_2^-$ ) and then to nitrate ( $\text{NO}_3^-$ ), which are less toxic than ammonia [3-5]. Yet, in farming system with a lack of aquatic plants, the accumulation of nitrogen compounds is faster than in a natural environment and causes problems with farming productivity.

Various adsorbents, such as zeolite [6-8], clays [9,10], ion exchange resins [11,12], modified activated carbons [13-16] and other materials [17-18], have been proposed for removal of ammonia since they have low cost and could remove ammonia by simple operation. In this work, the use of modified waste tire as adsorbent for ammonia is

reported. Although thermochemical conversion is widely used for the utilization of waste tire [19], waste tire has been used as an adsorbent that has been reported for the removal of heavy metals, arsenic compounds, organic molecules and oil [20-26]. Recently, Rungrodmitchai and Kotatha reported the modification of ground tire rubber (R-GTR) with ethylenediamine by microwave heating that gave the adsorbent for fluoride [27].

Through treatment of waste tire with oxidation agents, such as ozone, m-chloroperbenzoic acid, and periodic acid, nitrous oxide can cause the fractionation of the rubber and increase the oxygen content of the products [28-31]. From the viewpoint of chemical reaction, the oxidation of a double bond was reported to create oxygen-containing groups, such as carbonyl group ( $-\text{C}=\text{O}$ ) and carboxyl group ( $-\text{COOH}$ ) [32-34]. These functional groups are expected to be useful for the adsorption of cations and ammonia.

In this work, raw ground tire rubber (R-GTR) was modified by the oxidation system of  $\text{H}_3\text{PO}_4/\text{HNO}_3-\text{NaNO}_2$

to produce ammonia adsorbents. The characterization of the modified ground tire rubber (M-GTR) and the performance for ammonia adsorption were discussed.

## 2. Experimental

### 2.1 Raw Ground Tire Rubber (R-GTR)

R-GTR was purchased from Union commercial development company limited in Samut Prakan province, Thailand, nitric acid (65.0%), orthophosphoric (85.0%), sodium nitrite (97.0%), sodium hydroxide (98.0%), hydrochloric acid (37.0%), phenol crystals RPE (37.0%), sodium hypochlorite (5-9%Cl), sodium nitroprusside (100.0%), tri-sodium citrate dehydrate (99.0%) and ammonia solution (30.0%) were purchased from Carlo Erba. All chemicals were reagent grade or analytical grade and used as received.

### 2.2 Preparation of modified ground tire rubber (M-GTR)

Approximately 1.0 g of raw material was added to 50 ml of nitric acid/phosphoric acid in a glass bottle with the ratio 1:3 (%v/v). Then, 0.7 g of NaNO<sub>2</sub> (1.4%w/v) was added. After mixing all of the reactants, reddish fumes instantaneously occurred. Afterward, the glass bottle was capped and shaken with a speed of 80 rpm in a water bath shaker at 30°C for 96 hours. The obtained samples (M-GTR) were washed with distilled water until the filtrate reached pH 7. Then, M-GTR was dried at 105°C for 2 hours. Then, M-GTR was immersed in 500 ml of 0.1 M hydrochloric acid solution for 1 hour, washed with distilled water, and dried at 105°C for 2 hours before characterization.

### 2.3 Field emission scanning electron microscopy (FESEM)

The FESEM model JSM-7800F from JEOL at 5 kV with 1000x magnification was used to analyze the morphology of the obtained samples.

### 2.4 BET surface area analysis

BET analyzer model 3Flex from Micromeritics, USA was used to analyze the surface area. The pre-degassing and degassing process were performed by heating at 50°C for 60 min and 90°C for 1440 min, respectively. After that the obtained samples were analyzed by N<sub>2</sub> adsorption technique.

### 2.5 Ammonia adsorption

Approximately 100 mg of the sample were added to 20 ml of the ammonia solution with a known concentration (100, 200, 300, and 400 ppm). The mixture was shaken in a water bath shaker at room temperature for equilibrium time (360 minutes). Afterward, 10 ml of the supernatant was taken, and 0.5 ml of phenol solution, 0.5 ml of sodium nitroprusside solution, and 1 ml of oxidizing reagent were added to the sample. Then, the mixture solution was left for 1 hour before measuring absorbance at 630 nm by using UV-VIS spectrophotometer model U-2900 of Hitachi. The percentage adsorption and the quantity adsorbed (*q<sub>e</sub>*) were determined using the equation 1 and 2, respectively.

$$\%Adsorption = \frac{C_0 - C_e}{C_0} \times 100 \quad (1)$$

and the quantity adsorbed (*q<sub>e</sub>*) was determined as follows:

$$q_e \text{ (mg / g)} = \frac{C_0 - C_e}{m} \times V \quad (2)$$

where *q<sub>e</sub>* is the adsorption at equilibrium (mg/g), *C<sub>0</sub>* and *C<sub>e</sub>* are the initial and equilibrium concentration of the solution (mg/L), *V* is the volume of the solution (L) and *m* is the weight (g) of the sample.

## 3. Results and discussion

### 3.1 Morphology analysis

The morphology of R-GTR and M-GTR analyzed by FESEM are shown in figure 1. FESEM images demonstrated that the porosity of R-GTR increased after the modification.

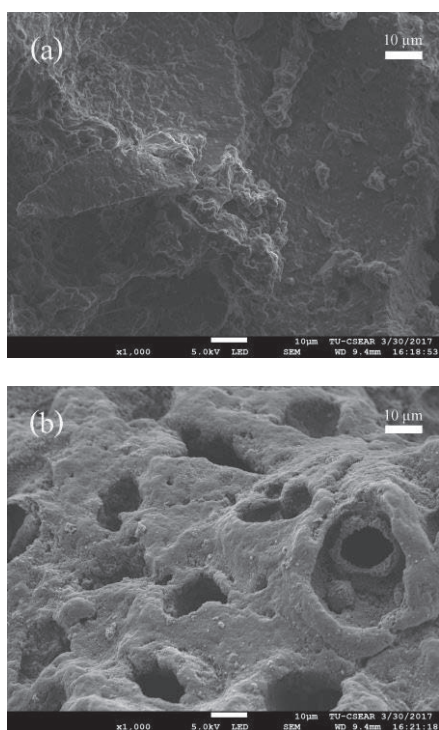


**Figure 1** FESEM images with 1000x magnification of (a) R-GTR and (b) M-GTR.

### 3.2 BET surface analysis

The surface area of R-GTR and M-GTR analyzed by BET surface area analysis that is listed in Table 1. The results revealed that the surface area of R-GTR and M-GTR were 2.57 and 10.37 m<sup>2</sup>/g, respectively. It was found that M-GTR was as large as 5 times that of R-GTR, which supported the results of the FESEM analysis.

**Table 1** The surface area of R-GTR and M-GTR from BET surface area analysis.

Sample	Surface area (m <sup>2</sup> /g)
R-GTR	2.57
M-GTR	10.37

### 3.3 Ammonia adsorption kinetics

The time dependence of the ammonia adsorption at a concentration of 1000 ppm of M-GTR is shown in figure 2. The result showed that adsorption reached to equilibrium in 360 minutes.

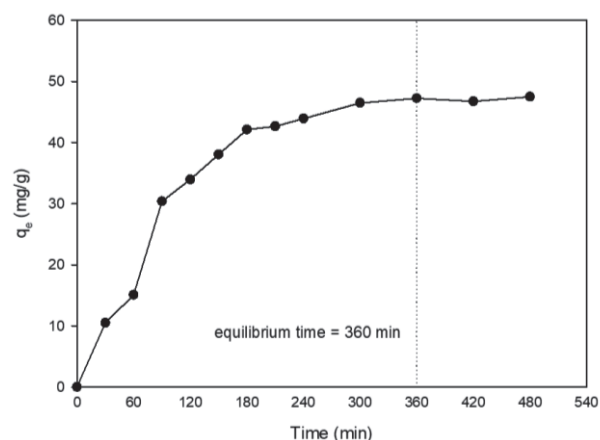


**Figure 2** The dependence of ammonia adsorption amount on adsorption times (initial concentration = 1000 ppm).

The kinetic study of ammonia adsorption by using M-GTR (the initial concentration of 1000 ppm) was analyzed the sample by the time interval of every 30 minutes for the first 240 minutes. After that, the sample was taken every 60 minutes until the concentration of ammonia reached an equilibrium. The kinetic data of ammonia adsorption was tested with two well-known kinetic models, which are pseudo-first order and pseudo-second order.

The pseudo-first order model is based on assumption that the rate of adsorption is proportional to the number of available sites. The linear form was expressed by following the equation 3 [35].

$$\log(q_e - q_t) = \log(q_e) - \frac{k_1 t}{2.303} \quad (3)$$

Where  $q_e$  and  $q_t$  are the adsorption capacity at equilibrium and at time (mg/g), respectively.  $t$  is contact time (min) and  $k_1$  is the rate constant of pseudo-first order (min<sup>-1</sup>). The values of  $k_1$  and  $q_e$  can be determined from slope and intercept of the linear plot between  $\log(q_e - q_t)$  versus  $t$ , respectively.

The pseudo-second order model assumes that the rate limiting step is controlled by chemical adsorption and the rate of adsorption is proportional to the second power of the available sites on the adsorbent. The linear form was

expressed by following the equation 4 [35].

$$\frac{t}{q_t} = \frac{1}{k_2 q_e^2} + \frac{t}{q_e} \quad (4)$$

Where  $k_2$  is the rate constant of pseudo-second order (g/mg·min). The values of  $k_2$  and  $q_e$  can be calculated from intercept and slope of the linear plot between  $t/q_t$  versus  $t$ , respectively.

The accuracy of adsorption kinetic was determined by the correlation coefficient ( $R^2$ ) and the standard deviation (S.D.) as shown in the equation 5 [36]. The smaller value of S.D. indicates a more suitable fitted model.

$$S.D. = \sqrt{\frac{\sum \left( \frac{q_{t,exp} - q_{t,cal}}{q_{t,exp}} \right)^2}{n-1}} \quad (5)$$

Where  $n$  is the number of experimental data points,  $q_{t,cal}$  (mg/g) is the calculated adsorption capacity at time and  $q_{t,exp}$  (mg/g) is the experimental adsorption capacity at time.

The linearized adsorption kinetics of pseudo-first order and pseudo-second order by using M-GTR are shown in figure 3. The kinetic parameters calculated from the linear plot are listed in table 2.

In accordance with the correlation coefficient ( $R^2$ ) values, M-GTR was fitted with pseudo-second order model better than pseudo-first order model. Besides, the calculated adsorption capacity from pseudo-second order model was closer to the experimental adsorption capacity than pseudo-first order model. Moreover, the standard deviation (S.D.) of pseudo-second order model was smaller than pseudo-first order model. From these results, it can be concluded that the ammonia adsorption by using M-GTR agreed with pseudo-second order model. This model indicated the ammonia adsorption was chemical adsorption.

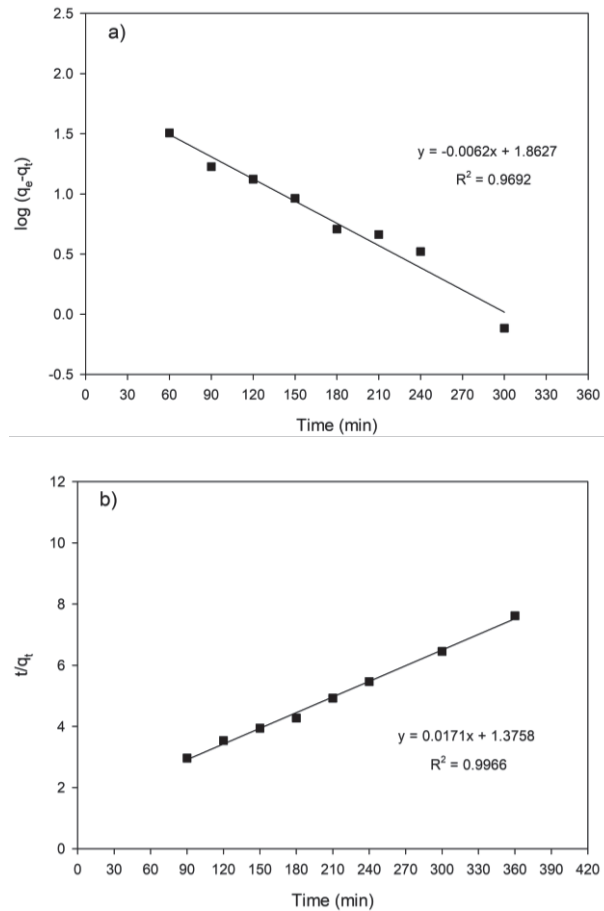


**Figure 3** The kinetic models for ammonia adsorption of M-GTR of a) pseudo-first order and b) pseudo-second order

**Table 2** The parameters for ammonia adsorption kinetics of M-GTR.

Kinetic models	parameters	M-GTR
pseudo-first order	$q_{exp}$ (mg/g)	47.24
	$q_{cal}$ (mg/g)	72.90
	$k_1$ ( $min^{-1}$ )	0.0143
	$R^2$	0.9692
	S.D.	0.2053
pseudo-second order	$q_{exp}$ (mg/g)	47.24
	$q_{cal}$ (mg/g)	58.48
	$k_2$ (g/mg·min)	0.0002
	$R^2$	0.9966
	S.D.	0.0899

### 3.4 Ammonia adsorption isotherms

The dependence of the removal efficiency (%) on ammonia concentration at equilibrium (360 minutes) by using R-GTR and M-GTR are shown in figure 4. The results from all ammonia concentrations showed that M-GTR had higher adsorption efficiency than R-GTR. The adsorption efficiency decreased when ammonia concentration increased. It was explained that increase of ammonia concentration increased the mass transfer rate but the active site on the adsorbent surface was limited by the amount of adsorbent. Consequently, the adsorption efficiency did not increase. At 100 ppm, the maximum adsorption efficiency of R-GTR and M-GTR was 36.15% and 22.05%, respectively.

The ammonia adsorption data of R-GTR and M-GTR were tested with Langmuir and Freundlich isotherms. Langmuir isotherm assumes that the monolayer adsorption for homogeneous surfaces. The linear form was expressed by the following equation 6 [37].

$$\frac{1}{q_e} = \frac{1}{q_m K_L C_e} + \frac{1}{q_m} \quad (6)$$

Where  $q_e$  is adsorption capacity at equilibrium (mg/g),  $C_e$  is the concentration of solution at equilibrium (mg/L),  $K_L$  is Langmuir equilibrium constant (L/mg) and  $q_m$  is the maximum adsorption capacity on surface in monolayer form of adsorbent (mg/g). The values of  $q_m$  and  $K_L$  can be calculated from intercept and slope of the linear plot between  $1/q_e$  versus  $1/C_e$ , respectively.

Freundlich isotherm assumes that the multilayer adsorption for heterogeneous surfaces. The linear form was expressed by the following equation 7 [37].

$$\log(q_e) = \log(K_F) + \frac{1}{n} \log(C_e) \quad (7)$$

Where  $q_e$  is the adsorption capacity at equilibrium (mg/g),  $C_e$  is the concentration of solution at equilibrium (mg/L),  $K_F$  is Freundlich equilibrium constant (mg/g)  $(L/mg)^{1/n}$  and  $n$  is the degree of nonlinearity. The values of  $K_F$

and  $1/n$  can be determined from intercept and slope of the linear plot between  $\log q_e$  versus  $\log C_e$ , respectively.

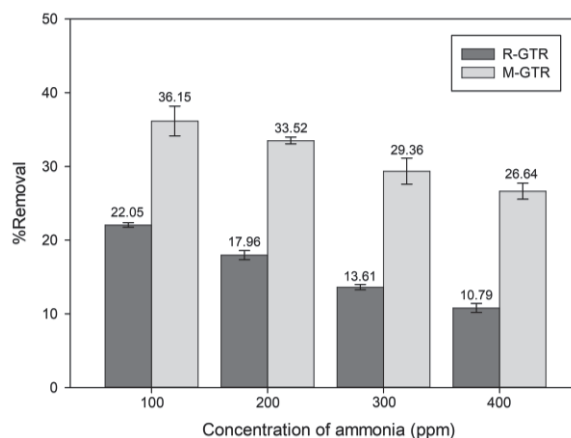


**Figure 4** The adsorption efficiency (%) of ammonia at equilibrium by using R-GTR and M-GTR.

The linearized adsorption of Langmuir and Freundlich isotherms by using R-GTR and M-GTR as adsorbents are shown in Figure 5. The Langmuir and Freundlich constants were calculated from the plot, as shown in Table 3.

According to Langmuir isotherm, the maximum ammonia adsorption capacities of R-GTR and M-GTR were 12.59 and 44.25 mg/g, respectively. The maximum capacity of M-GTR was higher than R-GTR because its surface contains more active sites than R-GTR. Those active sites were the oxygen-containing group from the oxidation reaction such as carbonyl group (-C=O) and carboxyl group (-COOH). Previous research reported that the carboxyl content of M-GTR was 1.58 mmol/g. On the other hand, R-GTR had no carboxyl group [33]. From the correlation coefficient ( $R^2$ ) values, M-GTR fitted well with both Langmuir and Freundlich isotherms, better than R-GTR. It could be explained that the ammonia adsorption by using M-GTR was physical and chemical adsorption. The first one related to the diffusion of ammonia ion into the pores of the adsorbent. The latter one may be occurred from the reaction between carboxyl group and ammonia ion is shown in Figure 6. The ammonia

ion attacked carboxyl group, where R-COOH gave H<sup>+</sup> (Lewis acid) and NH<sub>3</sub> accepted H<sup>+</sup> (Lewis base) and led to the formation of ammonium salt. Moreover, the maximum capacity was higher than the value of Amberjet 1200 Na and Dowax 50w-x8 [11,12] and zeolites [6-8].

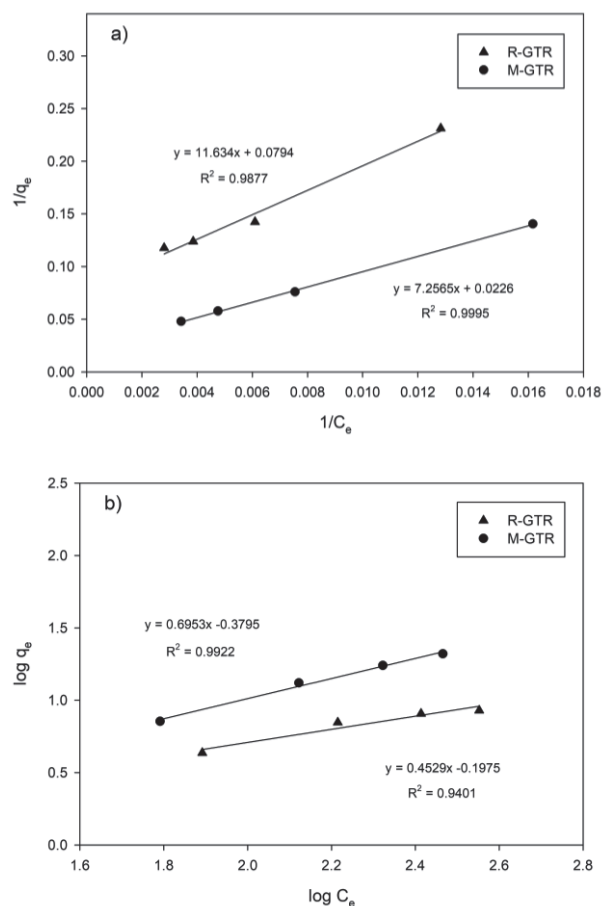


**Figure 5** The linearized ammonia adsorption plot of R-GTR and M-GTR of a) Langmuir and b) Freundlich isotherms.

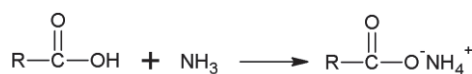


**Figure 6** The reaction between carboxyl group and ammonia.

The increase of surface area and carboxyl group caused the increase of ammonia adsorption capacity. It could be explained that the increase of surface area allowed physical adsorption of ammonia by pores. In addition, the increase of carboxyl group led to the chemical adsorption. Moreover, the

maximum ammonia adsorption capacity of M-GTR was large as 3.5 times of that of R-GTR, which confirmed that the effects of surface area and carboxyl group were important for ammonia adsorption.

**Table 3** The parameters for ammonia adsorption isotherm of R-GTR and M-GTR.

isotherm	parameters	R-GTR	M-GTR
Langmuir	$q_m$ (mg/g)	12.59	44.25
	$K_L$ (L/mg)	0.0068	0.0031
	$R^2$	0.9877	0.9995
Freundlich	$K_F$ (mg/g)(L/mg) <sup>1/n</sup>	0.6346	0.4173
	$n$	2.21	1.44
	$R^2$	0.9401	0.9922

#### 4. Conclusions

M-GTR was successfully prepared from R-GTR by using the oxidation reaction in an acid mixture from the HNO<sub>3</sub>/H<sub>3</sub>PO<sub>4</sub>-NaNO<sub>2</sub> system. However, the surface area increased after the modification by using oxidation reaction. In addition, the adsorption kinetic of M-GTR agreed with pseudo second-order model. Moreover, the adsorption isotherm of M-GTR was fitted well with both Langmuir and Freundlich isotherms, for which the maximum ammonia adsorption capacity was 44.25 mg/g.

#### 5. Acknowledgement

The authors would like to express our gratitude to the National Research Council of Thailand for financial support in fiscal year 2017 (Contract number: 31/2560).

#### 6. References

- [1] Camargo JA, Alonso Á. Ecological and toxicological effects of inorganic nitrogen pollution in aquatic ecosystems: a global assessment. *Environ Int.* 2006;32(6):831-49.

- [2] Smith VH, Tilman GD, Nekola JC. Eutrophication: impacts of excess nutrient inputs on freshwater, marine, and terrestrial ecosystems. *Environ Pollut.* 1999;100(1-3):179-96.
- [3] Bernet N, Delgenes N, Akunna JC, Delgenes J, Moletta R. Combined anaerobic-aerobic SBR for the treatment of piggery wastewater. *Water Res.* 2000;34(2):611-19.
- [4] Feng S, Xie S, Zhang X, Yang Z, Ding W, Liao X, et al. Ammonium removal pathways and microbial community in GAC-sand dual media filter in drinking water treatment. *J Environ Sci.* 2012;24(9):1587-93.
- [5] Siegrist H. Nitrogen removal from digester supernatant-comparison of chemical and biological methods. *Water Sci Technol.* 1996;34(1-2):399-406.
- [6] Turan M. Application of nanoporous zeolites for the removal of ammonium from wastewaters: A Review. In: Ünlü H, Horing N, Dabrowski J, editors. *Low-Dimensional and Nanostructured Materials and Devices.* Springer, Cham; 2016. p. 477-504.
- [7] Mazloomi F, Jalali M. Ammonium removal from aqueous solutions by natural Iranian zeolite in the presence of organic acids, cations and anions. *J Environ Chem Eng.* 2016;4(2):240-49.
- [8] Millar GJ, Winnett A, Thompson T, Couperthwaite SJ. Equilibrium studies of ammonium exchange with Australian natural zeolites. *J Water Process Eng.* 2016;9:47-57.
- [9] Ruiz R, Blanco C, Pesquera C, González F, Benito I, López JL. Zeolitization of a bentonite and its application to the removal of ammonium ion from waste water. *Appl Clay Sci.* 1997;12(1-2):73-83.
- [10] Soetardji JP, Claudia JC, Ju YH, Hriljac JA, Chen TY, Soetaredjo FE, et al. Ammonia removal from water using sodium hydroxide modified zeolite mordenite. *RSC Adv.* 2015;5:83689-99.
- [11] Jorgensen TC, Weatherley LR. Ammonia removal from wastewater by ion exchange in the presence of organic contaminants. *Water Res.* 2003;37(8):1723-28.
- [12] Chen PJ, Chua ML, Zhang B. Effects of competitive ions, humic acid, and pH on removal of ammonium and phosphorous from the synthetic industrial effluent by ion exchange resins. *Waste Manag.* 2002;22(7):711-19.
- [13] Yin CY, Aroua MK, Daud WMAW. Review of modifications of activated carbon for enhancing contaminant uptakes from aqueous solutions. *Sep Purif Technol.* 2007;52(3):403-15.
- [14] Halim AA, Aziz HA, Johari MAM, Ariffin KS. Comparison study of ammonia and COD adsorption on zeolite, activated carbon and composite materials in landfill leachate treatment. *Desalination.* 2010;262(1-3):31-5.
- [15] Vassileva P, Tzvetkova P, Nickolov R. Removal of ammonium ions from aqueous solutions with coal-based activated carbons modified by oxidation. *Fuel.* 2009;88(2):387-90.
- [16] Liu Z, Xue Y, Gao F, Cheng X, Yang K. Removal of ammonium from aqueous solutions using alkali-modified biochars. *Chem Speciation Bioavailability.* 2016;28(1-4):26-32.
- [17] Huang J, Kankanamge NR, Chow C, Welsh DT, Li T, Teasdale PR. Removing ammonium from water and wastewater using cost-effective adsorbents: A review. *J Environ Sci.* 2018;63:174-97.
- [18] Liu H, Dong Y, Liu Y, Wang H. Screening of novel low-cost adsorbents from agricultural residues to remove ammonia nitrogen from aqueous solution. *J Hazard Mater.* 2010;178(1-3):1132-36.
- [19] Labaki M, Jeguirim M. Thermochemical conversion of waste tyres-a review. *Environ Sci Pollut Res.* 2017;24(11):9962-92.
- [20] Bhatti IA, Ahmad N, Iqbal N, Zahid M, Iqbal M. Chromium adsorption using waste tire and conditions

- optimization by response surface methodology. *J Environ Chem Eng*. 2017;5(3):2740-51.
- [21] Gupta VK, Suhas, Nayak A, Agarwal S, Chaudhary M, Tyagi I. Removal of Ni(II) ions from water using scrap tire. *J Mol Liq*. 2014;190:215-22.
- [22] Knocke WR, Hemphill LH. Mercury (II) sorption by waste rubber. *Water Research*. 1981;15(2):275-82.
- [23] Wu B, Zhou MH. Recycling of waste tyre rubber into oil absorbent. *Waste Manag*. 2009;29(1):355-59.
- [24] Gupta VK, Ganjali MR, Nayak A, Bhushan B, Agarwal S. Enhanced heavy metals removal and recovery by mesoporous adsorbent prepared from waste rubber tire. *Chem Eng J*. 2012;197:330-42.
- [25] Imyim A, Sirithaweessit T, Ruangpornvisuti V. Arsenite and arsenate removal from wastewater using cationic polymer-modified waste tyre rubber. *J Environ Manage*. 2016;166:574-8.
- [26] Islam MT, Saenz-Arana R, Hernandez C, Guinto T, Ahsan MA, Bragg DT, et al. Conversion of waste tire rubber into a high-capacity adsorbent for the removal of methylene blue, methyl orange, and tetracycline from water. *J Environ Chem Eng*. 2018;6(2):3070-82.
- [27] Rungrodnimitchai S, Kotatha D. Chemically modified ground tire rubber as fluoride ions adsorbents. *Chem Eng J*. 2015;282:161-9.
- [28] Dubkov KA, Semikolenov SV, Ivanov DP, Babushkin DE, Panov GI, Parmon VN. Reclamation of waste tyre rubber with nitrous oxide. *Polym Degrad*. 2012;97(7):1123-30.
- [29] Cataldo F, Ursini O, Angelini G. Surface oxidation of rubber crumb with ozone. *Polym Degrad Stab*. 2010;95(5):803-10.
- [30] Cao XW, Luo J, Cao Y, Yin XC, He GJ, Peng XF, et al. Structure and properties of deeply oxidized waste rubber crumb through long time ozonisation. *Polym Degrad Stab*. 2014;109:1-6.
- [31] Sadaka F, Campistron I, Laguerre A, Pilard JF. Controlled chemical degradation of natural rubber using periodic acid: Application for recycling waste tyre rubber. *Polym Degrad Stab*. 2012;97(5):816-28.
- [32] Semikolenov SV, Nartova AV, Voronchikhin VD, Dubkov KA. New type of liquid rubber and compositions based on it. *Environ Sci Pollut Res Int*. 2014;21(21):12163-9.
- [33] Rungrodnimitchai S, Mayod S, Tanasarn S. The Utilization of Ground Tire Rubber as Ion Exchange Materials. *Defect Diffus Forum*. 2018;382:352-6.
- [34] Rungrodnimitchai S, Hiranphinyophat S. Oxidation of Palm Shell Coal Using HNO<sub>3</sub>/H<sub>3</sub>PO<sub>4</sub>-NaNO<sub>2</sub> System for Adsorbents. *Defect Diffus Forum*. 2018;382:312-7.
- [35] Netzahuatl- Muñoz AR, Cristiani- Urbina MdelC, Cristiani-Urbina E. Chromium biosorption from Cr(VI) aqueous solutions by cupressus lusitanica bark: kinetics, equilibrium and thermodynamic studies. *PLoS One*. 2015;10(9):e0137086.
- [36] Cheung CW, Porter JF, McKay G. Sorption kinetic analysis for the removal of cadmium ions from effluents using bone char. *Water Res*. 2001;35(3):605-12.
- [37] Nethaji S, Sivasamy A, Mandal AB. Adsorption isotherms, kinetics and mechanism for the adsorption of cationic and anionic dyes onto carbonaceous particles prepared from Juglans regia shell biomass. *Int J Environ Sci Technol*. 2013;10:231-42.